Journal of Molecular Modeling (2020) 26: 289
https://doi.org/10.1007/s00894-020-04541-y

ORIGINAL PAPER

Narrow-energy gap conjugated polymers based on benzobisthiadiazole and thiadiazoloquinoxaline: DFT and TDDFT study

Pervin Ünal Civcir[1] · Ezgi Özen[1] · Can Karadeniz[2]

Received: 16 July 2020 / Accepted: 13 September 2020 / Published online: 27 September 2020

Abstract

Herein, the HOMO–LUMO energy gaps (Eg) and UV spectra of benzo[1,2-c:4,5-c']bis([1,2,5]thiadiazole (BBT) and [1,2,5]thiadiazolo[3,4-g]quinoxaline (TQ)-based donor–acceptor–donor type-conjugated polymers were computed by using density functional theory (DFT) and time-dependent density functional theory (TD-DFT) at B3LYP/6-31G(d,p) level. The donor groups consist of thiophene (TH), 3,4-ethylenedioxythiophene (EDOT), and 3,4-propylene dioxythiophene (ProDOT) units and the bisthiadiazole and thiadiazoloquinoxaline were chosen as electron acceptor groups. To examine the effects of the alkyl side chain on the molecular structure and Eg of the polymer, methyl groups were added at the 3,4-, 2,3-, and 3,3-positions of TH, EDOT, and ProDOT donor groups, respectively. Our calculated HOMO-LUMO energy gaps are in the range of 0.05 to 1.37 eV. The calculation results show that the energy gaps are in line with the available experimental values. The novel BBT and TQ derivatives with improved optical and electronic properties may find use in electronic applications.

Keywords TDTFT · Benzobisthiadiazole · Thiadiazoloquinoxaline · Thiophene · EDOT · ProDOT

Highlights
- A series of donor–acceptor–donor type polymers based on benzobisthiadiazole and thiadiazoloquinoxaline are modeled
- Modeled polymers have remarkably low HOMO-LUMO energy gap values, which are range from 0.05 to 1.37 eV.
- The novel ProDOT and all methyl derivatives of the studied oligomers with improved optical and electronic properties may be used in the electronic applications.
- DFT calculations give good results for the HOMO-LUMO gaps of this type of polymers

Electronic supplementary material The online version of this article (https://doi.org/10.1007/s00894-020-04541-y) contains supplementary material, which is available to authorized users.

✉ Pervin Ünal Civcir
pervin.unal.civcir@science.ankara.edu.tr

Ezgi Özen
ozenezgi@ankara.edu.tr

[1] Department of Chemistry, Faculty of Science, Ankara University, 06100 Ankara, Turkey

[2] İstanbul, Turkey

Introduction

The most commonly used method to synthesize and design new organic conductive polymers with a low band gap is the usage of the molecules with donor–acceptor–donor (D-A-D) repeat units. Thiophene (TH), 3,4-ethylenedioxythiophene (EDOT), and 3,4-propylenedioxythiophene (ProDOT) as donor groups and benzothiadiazole (BTD), benzobisthiadiazole (BBT), and thiadiazolo[3,4-*g*]quinoxaline (TQ) as acceptor groups are the most common examples of the D-A-D type of polymer. Recent reports show that some low band gap polymers with BBT and TQ moieties are synthesized and some of them present very good results in electronic applications. Their applications are light-emitting devices (LED), organic field-effect transistors (OFEDs), and solar cells [1–19]. In addition to the experimental studies, computational modeling and examination of donor–acceptor–donor type-conjugated polymers have also been performed to find materials with low-energy gap [20–26]. Computational studies greatly contribute to identifying HOMO-LUMO gaps and optical properties and supporting experimental results. Therefore, quantum chemical calculations play an important role in the development of new materials with desired

electronic and optical properties. If the correct functional and basis set is chosen, the calculation results are quite compatible with the experimental values of the band gap of the polymers.

Very recently, we reported the structures and HOMO-LUMO energy gaps of benzo[c][1,2,5]thiadiazole (BTD) bonded to the thiophene, EDOT or ProDOT units as a donor, based D-A-D type-conjugated polymers. We revealed that these conjugated polymers show low-energy gap values (1.28–2.21 eV) and their calculated values were in a good agreement with the previously reported experimental findings [26]. In this work, we wanted to see how the acceptor groups affect the HOMO-LUMO energy gap, and thus, we selected benzo[1,2-*c*;4,5-*c*-]bis[1,2,5]thiadiazole (BBT) and thiadiazolo[3,4-*g*-]quinoxaline (TQ) as the acceptor groups. For this aim, we designed new BBT and TQ polymers with low HOMO-LUMO energy gap, conducted a quantum chemical study based on DFT as well as TD-DFT, and compared our results with experimental values that can be found in the literature. We report the details of our structural and energetic results for 13 derivatives. The chemical structures of monomers studied in this report are shown in Fig. 1. Our D-A-D type-conjugated polymers consist of TH, EDOT, and ProDOT units with or without methyl substitutions as the donor. It is well known that the existence of alkyl groups on the polymer increases the solubility of polymers in different organic solvents. Thus, to determine the influence of the alkyl groups on the structure and energy gap of the examined oligomers, the methyl groups were added to the TH, EDOT, and ProDOT in the 3,4, 2,3, and 3,3 positions, respectively. Methyl groups were chosen to simplify the calculations considering the computing cost.

According to our literature search, the BBT and TQ polymers bonded to the thiophene and EDOT units, which are **P1a** [12–15], **P2a** [16, 17], **P4a** [14, 16, 18], and **P5a** [14], were previously synthesized with a performance on organic light-emitting devices, solar cells, chemo-sensor, organic photovoltaic devices, and OLEDs. But, only the HOMO-LUMO energies of the oligomer of **P1a** were calculated theoretically using B3LYP, LSDA, BHandHLYP, and M06-2X functional and 6-31G(d), 6-31G(d,p), or cc-PVTZ basis sets in the literature [20–22, 24]. To our knowledge, ProDOT (**P3a**, **P6a**, and **P6c**) and methyl derivatives (**P1b**, **P2b**, **P3b**, **P4b**, **P5b**, and **P6b**) of BBT and TQ monomers, oligomers, and polymers have not been studied experimentally and theoretically in the literature so far; these were investigated for the first time in this study.

Computational methods

All calculations in this study were done with Gaussian 09W software [27]. To prepare data for calculations and display the calculation results, GaussView 5.0.8 molecular visualization program was used [28]. In our work, we first determined the most stable conformers of monomers by conformational analysis. A monomer unit ($n = 1$, where n is the number of monomer units) studied in this work consists of an acceptor (BBT or TQ rings) and two identical donor groups (TH, EDOT, or

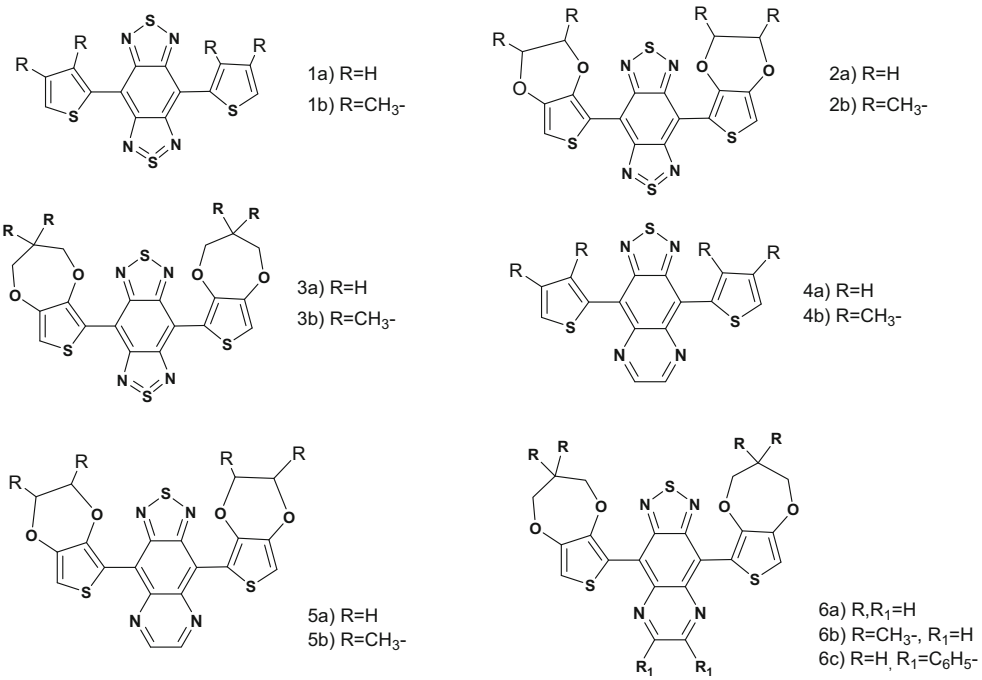

Fig. 1 Molecular structure of the studied monomers

ProDOT). The donor groups in a monomer unit have three possible conformers as cis-cis, trans-trans, and cis-trans relative to each other. Instead of studying all possible conformers of a monomer unit, we planned to continue our work with only the most stable conformer of the monomer that we can determine from conformation analysis. After determining the most stable configuration of all monomers, the most stable conformers for dimer and trimer structures were also determined. In the conformation analysis of the dimers, the rotation around the single bond connecting only two monomers is considered, while two rotations around the single bonds connecting each monomer units for the trimer systems are taken into account. The conformation analysis was not performed for tetramer and subsequent oligomers because of the calculation cost. The semi-empirical PM6 method [29] was applied to find the most stable conformations of each monomer, dimer, and trimer systems. In the second stage of calculations, the full geometry optimizations for only the most stable conformers of the monomers and oligomers were performed using the DFT [30, 31] in the gas phase. All molecular geometries were optimized with the B3LYP functional [32, 33] and 6-31G(d,p) basis set [34] and without any symmetry constraints. This level of theory was chosen since it gave a very good result for similar systems in our previous work and reduce the computational cost due to the large size of the oligomers [34].

The same level of theory was used to obtain the highest occupied molecular orbital (HOMO) and lowest unoccupied molecular orbital (LUMO) energies for all monomers and oligomers ($n = 1$ to 5). Using these calculated orbital energy values, the HOMO–LUMO energy gap (E_g), which is the difference between HOMO and the LUMO energy levels ($E_g = E_{LUMO} - E_{HOMO}$), was determined for all monomer and oligomer units. Then, the E_g values of the monomer and oligomers were plotted against the reciprocal of the oligomer length ($1/n$). The E_g value of the polymer was obtained by extrapolating the line of best fit. In the last step of our calculations, time-dependent density functional theory (TDDFT) computations were performed by using the same level of theory and basis set to the optimized structures. In this study, only the main transitions of each molecule were considered. The main excited state transitions (E_{exc}) correspond to transitions from HOMO to LUMO. Also, the exciton binding energy (E_b), which is the difference between the HOMO−LUMO energy gap and excitation energy, was estimated.

Finally, we compared the calculated energy gaps with the experimental and previously calculated results when available and evaluated the reliability of the method used in estimating E_g values of the studied compounds. Our results obtained from the DFT/TDDFT calculations and their comparisons with the experimental and theoretical values are explained in the following sections.

Results

By our purpose, the structural and electronic characteristics of the monomers and oligomers are examined computationally and the results obtained from the calculations are given below. It is well known that the band gap of the conjugated systems directly related to the molecular structure. Therefore, before explaining the HOMO-LUMO energy gaps and absorption spectra of the studied compounds, we discussed the calculation results related to the structural parameters of monomers and oligomers.

Structural properties

The inter-ring C–C dihedral angles (φ), which is one of the structural parameters, are important because it provides for limiting the delocalization of π-electrons along the conjugated chain and decreasing the HOMO-LUMO energy band. To determine the most stable conformer and its dihedral angle, the conformation analysis was performed using a semi-empirical PM6 method for all structures from monomer to trimer. The atom-numbering scheme used to illustrate the dihedral angles of the oligomers is shown in Fig. 2. The most stable conformers of all monomers, dimers, and trimers obtained from the conformation analysis are shown in Fig. 1Sa-1Sm in Supporting Information. The results of the conformation analysis for all unsubstituted monomers indicate that all torsion angles between unsubstituted TH, EDOT, or ProDOT and acceptor group (BBT or TQ) are 0° or almost 0° and the most stable conformations are planar or almost planar (Table 1). For all BBT monomers, the sulfur atoms of the TH, EDOT, or Pro-DOT rings were positioned trans to each other. In the case of all TQ monomers, it is just the opposite of that above, that is, the sulfur atoms of TH, EDOT, or Pro-DOT were in a cis position to each other. However, the sulfur atom of the thiadiazole ring of TQ was in trans position to the sulfur atom of each donor group (TH, EDOT, or Pro-DOT). Methyl substituted derivatives except P5b monomer have a smaller torsional energy barrier and are slightly away from planarity due to the steric effect of the methyl groups.

After determining the most stable conformations for all monomers, the conformation analysis of the dimers was performed using the data of the monomer conformers. The torsion angles (φ_3) of all dimers, except **P1a**, **P1b**, **P4a**, and **P4b** dimers, which are the thiophene derivatives, are almost 0° and the sulfur atoms of the TH, EDOT, or ProDOT rings connecting two monomer units are positioned opposite to each other (trans conformation). Calculation results obtained for the trimers are the same as those obtained for the dimer systems. That is, the inter-ring dihedral angles (φ_3 and φ_6) of all trimers, except **P1a**, **P1b**, **P4a**, and **P4b**, are almost 180° and the sulfur atoms of TH, EDOT, or ProDOT rings connecting the monomer units are located on different sides with respect to each other (trans conformations). In the case of longer oligomers ($n = 4$ and 5 in

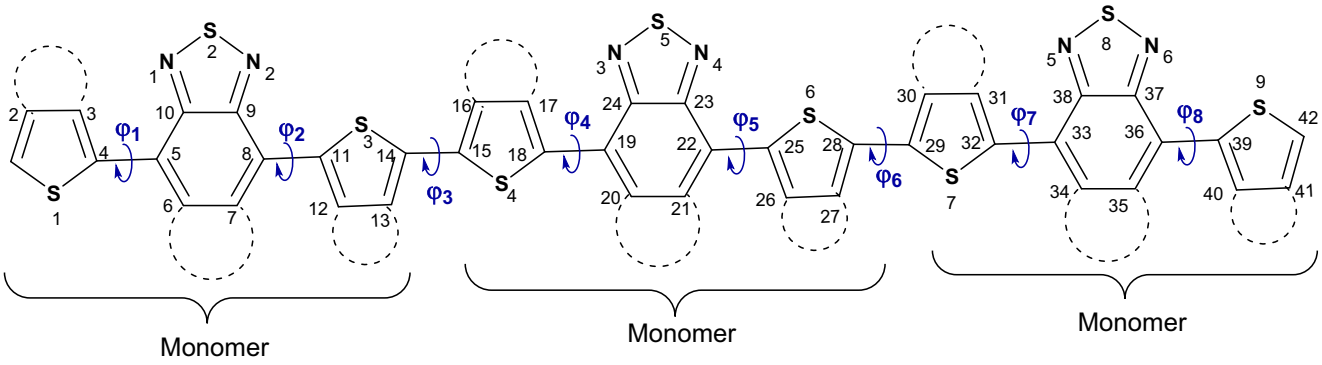

Fig. 2 Atom numbering scheme used to indicate the inter-ring dihedral angles (denoted as φ_i) for the oligomers ($n = 3$)

general), we continued the calculations assuming that the trans conformers would be the most stable structure.

In the next step, the full geometry optimization was performed by using DFT for the most stable conformers of all monomers and oligomers. The optimized molecular structures of all monomers are presented in Fig. 3 together with intramolecular interaction distances, and the optimized structures of all oligomers ($n = 2$ to 5/6) are given in Fig. 2Sa-2Sm in Supporting Information. The dihedral angles obtained from the geometry optimization calculations are also shown in Table 1. The geometry optimization results indicate that the dihedral angles (φ_1, φ_2, φ_3, φ_4, φ_5, φ_6, φ_7, φ_8) of all oligomers, except **P1a**, **P1b**, **P2b**, **P3b**, **P4a**, and **P4b**, are all equal to 180° or almost 180°, and most of the oligomers have a planar or almost planar structure showing a strong π-electron delocalization in the main chain. **P1a** and **P2a** monomers have crystal structure data in the literature and we compared our findings to the experimental values. X-ray analysis of the **P1a** monomer revealed that this monomer has the planar conformation and the dihedral angles between the thiophene rings and the central BBT unit are only 0° [13, 14]. The calculated dihedral angles for **P1a** monomer are in very good agreement with these experimental values. However, there is a difference between the experimentally determined value (53°) and the computed value (0.6°) of dihedral angles between EDOT and BBT rings in **P2a** monomer. This can be attributed to the magnitude of steric interactions between the nitrogen atoms of BBT and EDOT's oxygen atoms in the solid phase because there are strong molecular interactions in this phase.

The planar monomer systems studied are stabilized in the planar form by the intramolecular interactions between the donor group's hydrogen, sulfur or oxygen atoms, and nitrogen atoms of the acceptor groups. There is no steric repulsion between adjacent heterocyclic rings of all monomer systems and the interaction distances are very short. As can be seen from Fig. 3, the **P1a**, **P1b**, **P2a**, **P3a**, **P4a**, **P5a**, **P5b**, **P6a**, **P6b**, and **P6c** monomers have the symmetrical intramolecular interaction distances (**H… N**, **S… N**, or **O… N)** and the values are very close to the values observed in similar systems [26, 35].

In this part, the results related to the calculated bond lengths of the monomers and oligomers are discussed. The atom-numbering scheme used to show the bond lengths of all monomers is presented in Fig. 4 and the results of the geometry optimization using B3LYP/6-31G (d,p) for the monomers are given in Table 2. The selected bond lengths for the dimer and trimers are given in Table S1 in Supporting Information. As can be seen from Table 2, for all monomers, the C–C single bond lengths in the main chain are shorter than C–C single bonds and larger than C=C double bonds. The calculated S–N and C–N bond lengths of thiadiazole rings in BBT monomers are approximately 1.66 and 1.36 Å, respectively. Similarly, the computed S–N and the C–N bonds of thiadiazole rings of TQ monomers are about 1.69 Å and 1.33 Å, respectively. The calculated C–N bond lengths of the quinoxaline ring are 1.31 and 1.42 Å. Due to the stronger delocalization of π-electrons, the calculated S–N and C–N bond lengths are found to be longer and shorter than the normal S=N (1.54 Å) and C=N (1.38 Å) bond lengths, respectively.

Since X-ray crystal structures of the **P1a** and **P2a** molecules are available in the literature, we compared the geometries computed using the DFT with the experimental values for these two molecules in Table 2. There are small differences between the calculated and the experimental bond lengths of these compounds and the maximum deviation are around 0.066 Å for C–C, S–N, and C–N bonds. This is because the experimental measurements are taken in the solid phase while the calculations are performed in the gas phase and it is well known that there are strong intermolecular interactions in the solid phase. Therefore, it can be concluded that the DFT-optimized geometry of the **P1a** and **P2a** monomers is in agreement with the experimental results.

The N–S–N bond of one of the thiadiazole rings in the BBT molecule is usually represented as a single bond while the second ring is denoted as double bonds in the form of N = S = N as shown in Fig. 1. This resonance structure of the molecule is more stable than other resonance forms. However, our calculation results for the larger oligomers showed that the N–S–N bonds in both thiadiazole rings of

Table 1 Torsion angles (°) of the monomers and oligomers (n = 1–3) calculated using the B3LYP/6-31G(d,p)

	P1a	P1b	P2a	P2b	P3a	P3b	P4a	P4b	P5a	P5b	P6a	P6b	P6c
n = 1													
φ_1	0.0 (0.1)	37.5 (29.9)	0.6 (0.3)	16.6 (10.8)	0.5 (0.1)	2.5 (0.1)	0.0 (0.1)	1.4 (0.0)	0.3 (0.9)	0.2 (0.9)	0.2 (2.9)	0.5 (2.9)	0.1 (0.0)
φ_2	0.0 (0.1)	37.5 (28.2)	0.6 (0.3)	26.3 (19.5)	0.5 (0.1)	2.5 (58.7)	0.0 (0.1)	51.7 (59.9)	0.3 (1.5)	0.2 (1.5)	0.2 (0.3)	0.5 (0.3)	0.8 (3.1)
n = 2													
φ_1	0.0 (0.0)	37.4 (37.5)	0.1 (0.1)	31.8 (29.7)	0.5 (11.5)	6.5 (6.4)	0.0 (0.0)	53.6 (0.1)	0.3 (0.3)	0.0 (0.0)	0.2 (0.2)	0.5 (45.5)	0.4 (0.4)
φ_2	0.1 (0.1)	35.4 (35.6)	0.6 (0.5)	12.1 (19.3)	0.5 (8.3)	23.3 (13.3)	0.1 (0.1)	0.2 (53.4)	0.3 (0.4)	0.3 (0.3)	2.3 (2.4)	1.6 (39.1)	12.7 (13.0)
φ_3	157.3 (160.0)	108.2 (116.2)	180.0 (180.0)	179.7 (179.8)	180.0 (180.0)	177.2 (178.8)	147.6 (150.0)	98.1 (90.0)	179.6 (177.1)	174.9 (175.5)	180.0 (180.0)	178.8 (179.5)	178.9 (180.0)
φ_4	0.1 (0.1)	38.2 (35.6)	0.6 (0.6)	19.3 (12.1)	0.5 (8.3)	0.9 (1.0)	0.1 (0.1)	0.2 (0.1)	0.3 (0.2)	0.8 (0.8)	2.4 (2.4)	1.6 (46.3)	6.8 (6.5)
φ_5	0.0 (0.0)	38.0 (37.5)	0.1 (0.1)	29.7 (31.8)	0.5 (11.5)	56.9 (55.0)	0.0 (0.0)	53.6 (53.4)	57.0 (57.0)	0.1 (0.1)	0.2 (0.2)	0.5 (52.0)	0.3 (0.4)
n = 3													
φ_1	0.0 (0.0)	38.1 (0.1)	1.0 (1.3)	9.1 (24.3)	15.8 (11.5)	2.6 (2.2)	0.0 (0.0)	53.7 (53.8)	0.3 (0.3)	0.1 (0.0)	0.2 (0.2)	0.5 (0.5)	1.0
φ_2	0.1 (0.1)	38.0 (0.1)	1.2 (1.7)	53.8 (29.0)	9.7 (8.4)	12.9 (20.6)	0.1 (0.1)	0.2 (1.9)	0.2 (0.4)	0.2 (0.2)	2.3 (2.3)	1.5 (1.4)	1.8
φ_3	157.4 (160.0)	108.1 (157.4)	179.9 (177.7)	179.3 (180.0)	176.9 (180.0)	178.2 (170.6)	147.8 (155.8)	97.7 (97.0)	179.6 (167.1)	174.7 (175.5)	175.9 (180.0)	178.0 (170.5)	158.1
φ_4	0.1 (0.1)	35.3 (0.2)	0.2 (0.4)	2.4 (3.4)	1.3 (8.4)	1.5 (1.6)	0.1 (0.1)	0.1 (2.2)	0.2 (0.4)	0.8 (0.9)	2.3 (2.4)	1.6 (62.5)	7.9
φ_5	0.2 (0.2)	35.3 (0.2)	0.1 (0.4)	60.0 (59.43)	1.0 (11.5)	9.5 (9.9)	0.0 (0.1)	53.9 (51.6)	0.4 (0.0)	0.5 (0.5)	2.2 (2.4)	1.7 (1.8)	4.4
φ_6	157.4 (155.3)	108.1 (157.4)	179.9 (179.0)	179.8 (179.0)	176.8 (180.0)	179.7 (178.8)	147.8 (151.9)	108.9 (108.2)	179.5 (147.1)	175.0 (174.7)	175.9 (180.0)	178.1 (179.5)	179.8
φ_7	0.1 (0.1)	38.0 (0.1)	1.2 (1.0)	2.0 (2.3)	9.8 (11.5)	1.9 (2.6)	0.1 (0.1)	53.6 (52.2)	0.2 (0.4)	0.8 (0.7)	2.3 (2.3)	1.4 (2.0)	14.20
φ_8	0.0 (0.0)	38.0 (0.0)	1.0 (0.9)	60.1(59.2)	15.7 (8.4)	20.7 (12.9)	0.0 (0.0)	0.7 (2.2)	58.1 (57.3)	0.0 (0.0)	0.2 (0.2)	0.5 (56.5)	0.5

φ_1: S(1)-4-5-6, φ_2: 7-8-11-S(3), φ_3: S(3)-14-15-S(4), φ_4: S(4)-18-19-20, φ_5: 21-22-25-S(6), φ_6: S(6)-28-29-S(7), φ_7: S(7)-32-33-34 φ_8: 35-36-39-S(8)

Figures in brackets show the results of scan analysis

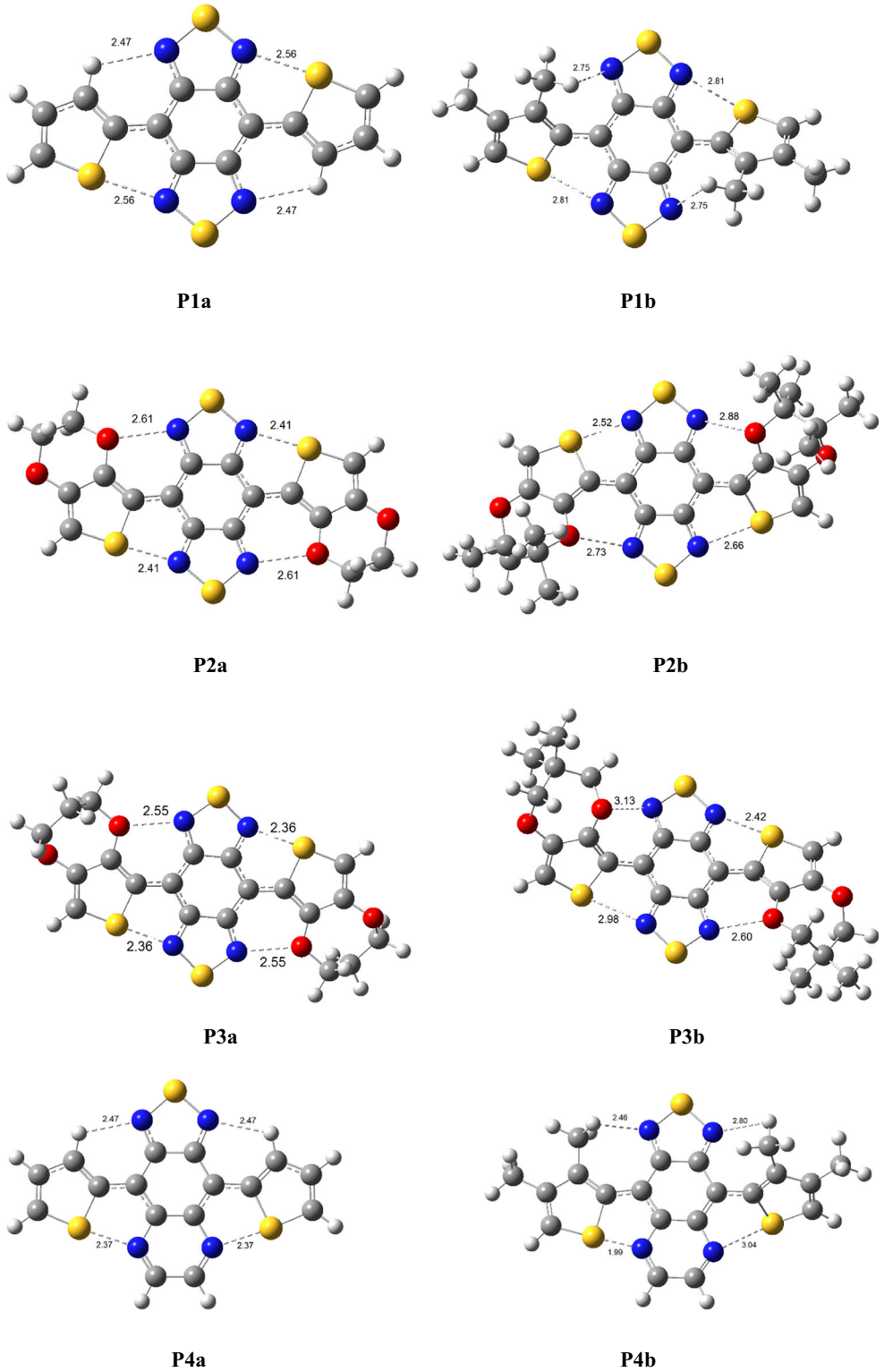

Fig. 3 The optimized geometries of all monomers along with intramolecular interaction distances

BBT are single bonds and these resonance structures are more stable. Both BBT and TQ oligomers are quinoid type acceptors as given in Fig. 5. Since the more stable 1,2,5-thiadiazole rings are in quinoid form, a strong contribution of this form for the studied molecules is expected, and the quinoid contribution of the BBT unit is larger than the TQ unit.

The bridge bond lengths (*L*B) were determined to explain the molecular structures of the studied monomer oligomers.

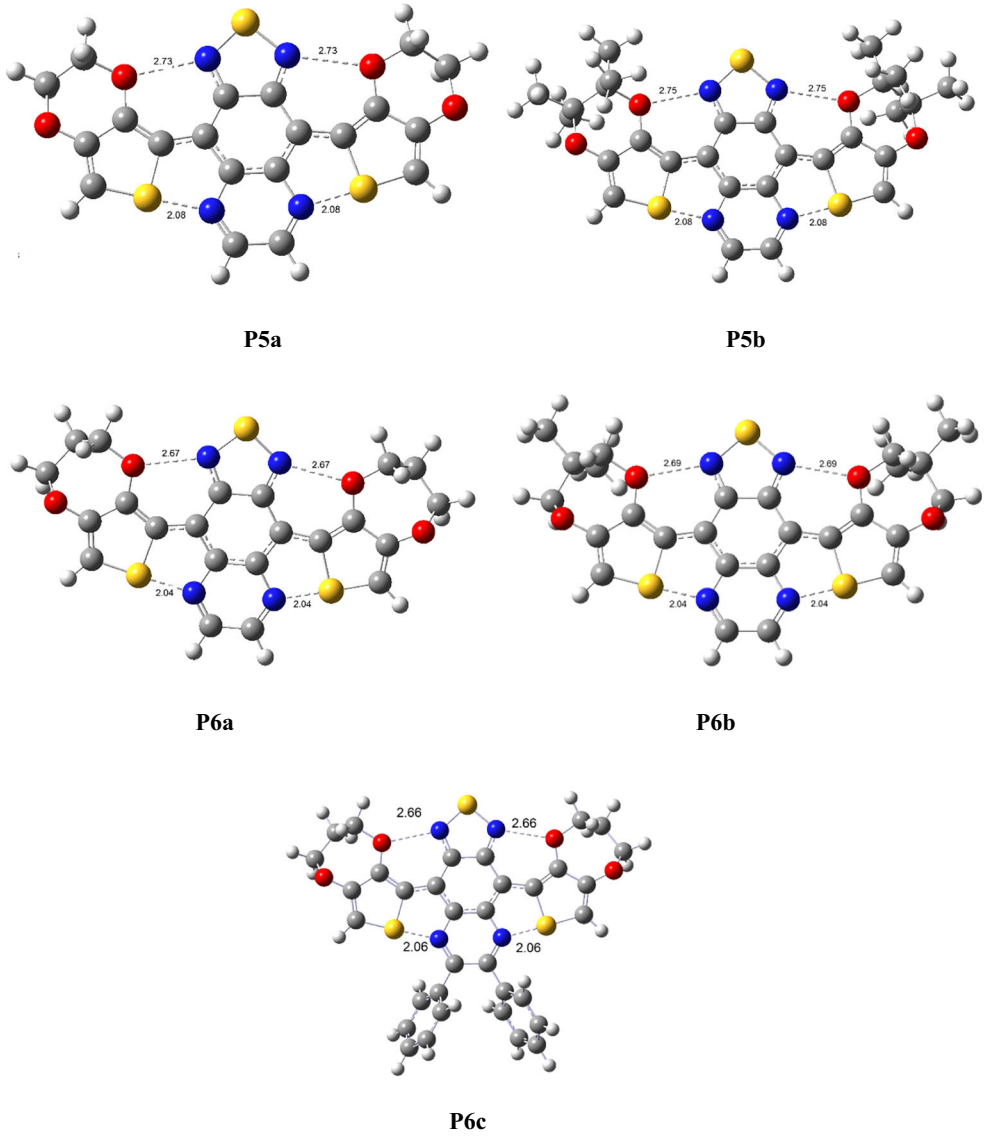

Fig. 3 (continued)

The *L*B values of the calculated oligomers were found in the range of 1.41–1.44 Å, indicating that *L*B is almost 0.13 Å shorter than experimentally measured bond length of the C–C bond (1.54 Å). The bond length reduction shows that all studied monomers and oligomers have a partial double-bond property. This is because the partial double-bond property of the bridge bond between the donor and acceptor units strengthens and shortens the bridge bond length.

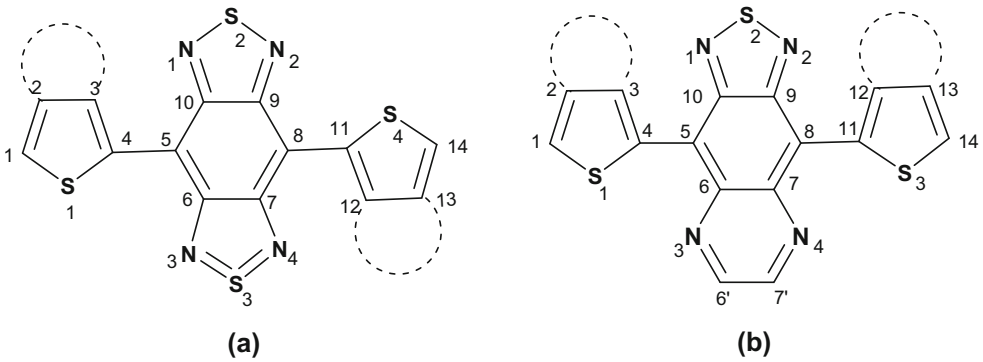

Fig. 4 Atom numbering scheme of the BBT (**a**) and TQ (**b**) monomers

Table 2 Selected bond lengths (Å) of all monomers calculated using the B3LYP/6-31G(d,p) along with the experimental values

Monomer	**P1a**		**P1b**	**P2a**		**P2b**	**P3a**	**P3b**	**P4a**	**P4b**	**P5a**	**P5b**	**P6a**	**P6b**	**P6c**
Bond	Calc.	Exp.[a]	Calc.	Calc.	Exp. [c]	Calc.	Calc.	Calc.	Calc.	Calc.	Calc.	Calc.	Calc.	Calc.	Calc.
S(1)–C(1)	1.735		1.731	1.743		1.743	1.736	1.737	1.737	1.743	1.759	1.761	1.754	1.755	1.756
S(1)–C(4)	1.760		1.756	1.778		1.773	1.776	1.757	1.767	1.809	1.806	1.808	1.808	1.808	1.810
C(1)–C(2)	1.364		1.365	1.357		1.358	1.361	1.364	1.363	1.360	1.352	1.351	1.355	1.354	1.355
C(2)–C(3)	1.439		1.460	1.462		1.464	1.463	1.461	1.439	1.46	1.464	1.466	1.466	1.465	1.464
C(3)–C(4)	1.372		1.374	1.374		1.375	1.381	1.371	1.370	1.377	1.369	1.37	1.376	1.375	1.38
C(4)–C(5)	1.436	1.471	1.441	1.430		1.430	1.429	1.440	1.438	1.431	1.427	1.426	1.425	1.425	1.418
C(5)–C(6)	1.416	1.405[a] 1.406[c]	1.416	1.420	1.405	1.421	1.421	1.411	1.389	1.398	1.391	1.391	1.392	1.392	1.399
C(5)–C(10)	1.415	1.405[a,b]	1.413	1.416		1.416	1.417	1.415	1.448	1.451	1.449	1.451	1.451	1.451	1.449
C(6)–C(7)	1.493		1.497	1.494		1.496	1.494	1.502	1.453	1.453	1.442	1.443	1.441	1.441	1.452
C(7)–C(8)	1.415		1.413	1.416		1.416	1.417	1.416	1.389	1.383	1.391	1.391	1.392	1.392	1.383
C(8)–C(9)	1.416		1.416	1.420	1.412	1.416	1.421	1.427	1.448	1.449	1.449	1.451	1.451	1.451	1.450
C(9)–C(10)	1.493	1.464	1.497	1.494	1.447	1.499	1.494	1.492	1.500	1.507	1.514	1.517	1.517	1.517	1.506
C(10)–N(1)	1.364	1.352[a] 1.350[b]	1.364	1.361		1.361	1.360	1.360	1.336	1.332	1.330	1.328	1.328	1.328	1.330
N(1)–S(2)	1.655	1.596 [a,b]	1.656	1.656		1.656	1.657	1.665	1.684	1.686	1.689	1.692	1.691	1.691	1.689
S(2)–N(2)	1.657		1.655	1.663	1.603	1.661	1.665	1.663	1.684	1.688	1.689	1.692	1.691	1.691	1.693
N(2)–C(9)	1.365	1.345	1.365	1.364	1.365	1.363	1.364	1.360	1.336	1.333	1.330	1.328	1.328	1.328	1.331
C(6)–N(3)	1.365	1.352[b]	1.364	1.364		1.361	1.364	1.363	1.420	1.417	1.417	1.417	1.417	1.416	1.413
N(3)–S(3)	1.657	1.590[b]	1.655	1.663		1.663	1.665	1.660	-	-	-	-	-	-	-
S(3)–N(4)	1.655		1.656	1.656		1.661	1.657	1.652	-	-	-	-	-	-	-
N(3)–C(6′)	-		-	-		-	-	-	1.306	1.308	1.310	1.310	1.310	1.310	1.314
C(6′)–C(7′)	-		-	-		-	-	-	1.479	1.477	1.478	1.477	1.477	1.477	1.494
C(7′)–N(4)	-		-	-		-	-	-	1.306	1.304	1.310	1.310	1.310	1.310	1.310
N(4)–C(7)	1.364		1.364	1.361		1.360	1.360	1.362	1.420	1.422	1.417	1.417	1.417	1.416	1.419
C(8)–C(11)	1.436		1.441	1.431	1.463	1.433	1.429	1.424	1.438	1.446	1.427	1.426	1.425	1.425	1.442
C(11)–C(12)	1.372		1.374	1.374	1.372	1.371	1.381	1.384	1.37	1.371	1.369	1.37	1.376	1.375	1.374
C(12)–C(13)	1.439		1.46	1.461	1.420	1.464	1.463	1.462	1.439	1.461	1.464	1.466	1.466	1.465	1.465
C(13)–C(14)	1.364		1.365	1.357	1.356	1.359	1.361	1.361	1.363	1.365	1.352	1.351	1.355	1.354	1.363
C(14)–S(4)	1.735		1.731	1.743		1.743	1.736	1.735	-	-	-	-	-	-	-
C(11)–S(4)	1.760		1.756	1.778		1.768	1.776	1.773	-	-	-	-	-	-	-
C(14)–S(3)	-		-	-		-	-	-	1.737	1.733	1.759	1.761	1.754	1.755	1.735
C(11)–S(3)	-		-	-		-	-	-	1.767	1.751	1.806	1.808	1.808	1.808	1.752

[a] Taken from Ref [13]

[b] Taken from Ref [19]

[c] Taken from Ref [17]

One way to express the correct geometry of molecules is bond lengths, it is necessary to identify single- and double-bond changes especially in conjugated systems. The biggest is the bond length alternation (BLA), the larger the band gap becomes. The evaluated BLA values are given monomers, dimers, and trimers in Table S2 in Supporting Information. Our results show that all the dimer and trimer structures, except **P3b**, have almost the same BLA values and **P3b** does not follow up on the alternation pattern of single and double bonds. However, the BLA values of the trimers for **P1b** and **P4b**, which are methyl-substituted bis-thiophene derivatives, are larger than the other oligomers. The charge delocalization of the oligomers (**P1a**, **P2a**, **P2b**, **P3a**, **P4a**, **P5a**, **P5b**, **P6a**, **P6b**, and **P6c)** on the main chain is quite strong, so we expect the energy gap values of these oligomers to be smaller. On the other hand, the charge delocalization of **P1b** and **P4b** oligomers is relatively poor, and their E_g values are expected to be higher than other oligomers.

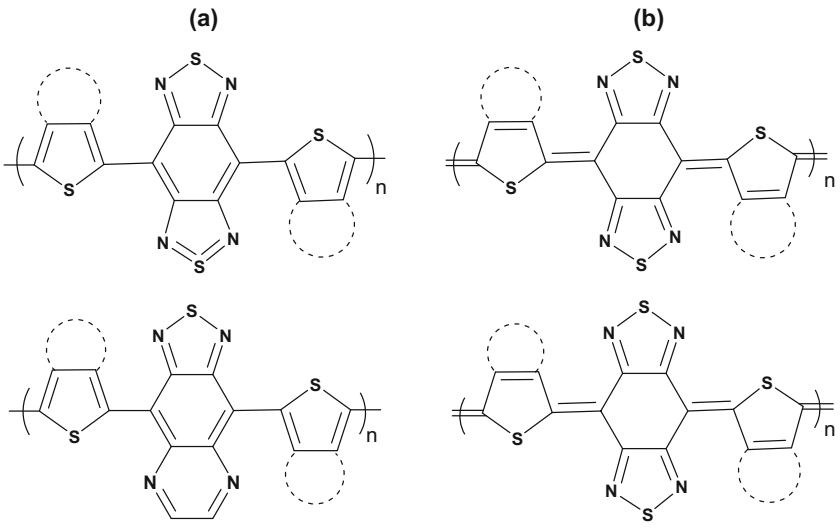

Fig. 5 Aromatic (**a**) and quinoid (**b**) structures of the studied molecules

HOMO-LUMO energy gap

To determine the HOMO-LUMO energies and energy gaps of the studied monomers and oligomers, the orbital energies were computed by the DFT at the B3LYP/6-31G (d,p) level in the gas phase using the previously optimized structures. The HOMO and LUMO graphs show π molecular orbital characteristics and the electronic cloud distribution of both molecular orbitals. The contour diagrams of HOMO and LUMO orbitals of all monomers are shown in Fig. 6. From the contour diagrams of the molecular orbitals, the electron charge density of the unsubstituted and methyl-substituted monomers' HOMO and LUMO orbitals shows very similar trends. Similarly, the electron distribution of HOMO and LUMO orbitals of the thiophene and EDOT derivatives bonded to BBT or TQ is almost the same. However, this differs in ProDOT derivatives. The LUMO molecular orbitals of all monomers are mostly localized over the BBT and TQ acceptor units. At the HOMO level, the electron charge density for thiophene and BBT-linked ProDOT derivatives spreads on the main chain, while the electron density for EDOT and TQ-bonded ProDOT derivatives is mainly localized on the donor groups. Simulated HOMO and LUMO molecular orbitals of all pentamers are presented in Fig. S3 in Supporting Information. From these graphs, it was observed that the results for the pentamers are very similar to those obtained for monomers. In general, at the HOMO level, the electron charge density of all pentamers was mostly on the main chain, while at the LUMO level, it was mainly on acceptor groups.

The computed E_{HOMO}, E_{LUMO}, and E_g, E_{exc} E_b values for the studied monomers and oligomers are given in Table 3 together with the experimental values that can be found in the literature. Using the computed E_g values of monomers and oligomers, the E_g values of the polymers were determined by linear regression and an extrapolation procedure, and obtained results are given in Fig. 7. The evaluated E_g values of the polymers are in the range of 0.05–1.37 eV and these values are within the band gap range of the semiconductor. As seen from Table 3, HOMO energies increase from monomer to pentamer while LUMO energies decrease, and consequently, band energies decrease.

As can be seen from Table 3, BBT polymers have smaller energy gap than the TQ analogs. This was expected since BBT is a strong electron-withdrawing molecule with two-hypervalent sulfur atoms. On the other hand, the HOMO-LUMO energy gap of the polymers containing thiophene (**P1a**, **P1b**, **P4a**, and **P4b)** was found to be larger than polymers containing EDOT or ProDOT. The thiophene oligomers deviated slightly from planarity (157.4° for **P1a**, 108.1° for **P1b**, 147.8° for **P4a**, and 97.7° for **P4b**, φ_3 values in trimers). Deviation from planarity affects the delocalization of π-electrons and increases the energy gap. Also, the E_g values of polymers with ProDOT (**P3a**, **P6a**, and **P6b**) are lower than the EDOT-containing analogs (**P2a**, **P5a**, and **P5b**), except **P2b**.

When we examine the effect of alkyl groups on the E_g value, we observed that the methyl groups had two different effects on the E_g values of the molecular group studied. The E_g values of methyl-substituted thiophene (**P1b** and **P4b)** and ProDOT (**P3b)** polymers increase compared with unsubstituted analogs due to the steric effects of methyl groups. On the other hand, the E_g values of EDOT analogs (**P2b**, **P5b**, and **P5b)** decrease due to the electron donor effects of the methyl groups. Also, the first group of molecules deviated from the planarity in their oligomers, while those in the second group retained their

Fig. 6 HOMO and LUMO contour graphs of all monomers

Monomer	HOMO	LUMO
P1a	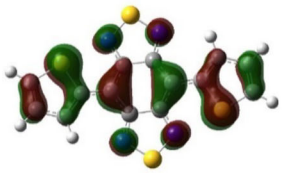	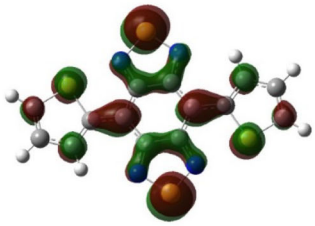
P1b	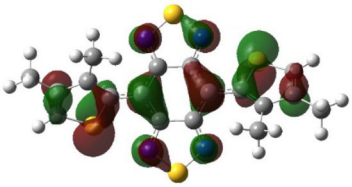	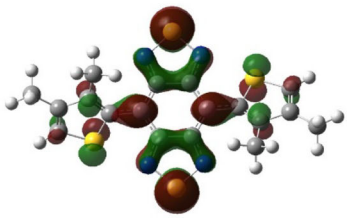
P2a	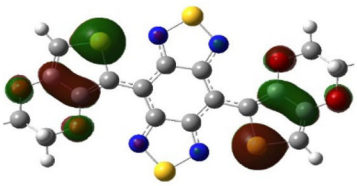	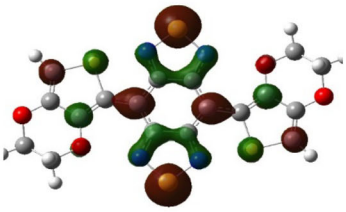
P2b	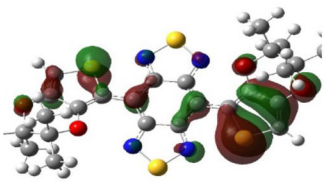	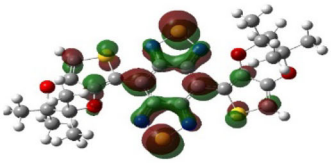
P3a	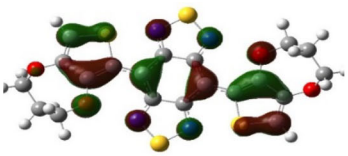	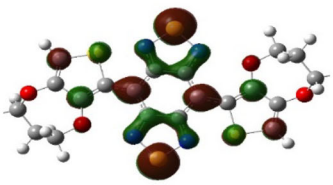
P3b	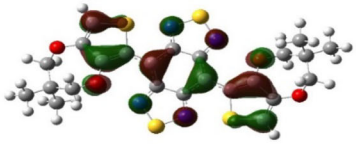	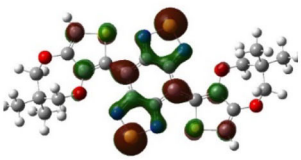

Fig. 6 (continued)

P4a	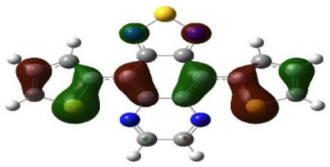	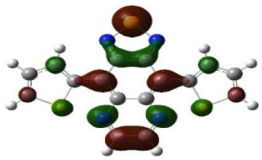
P4b	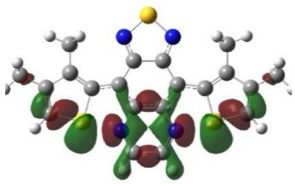	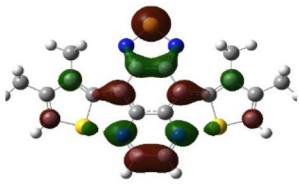
P5a		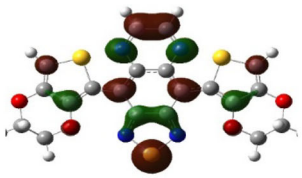
P5b	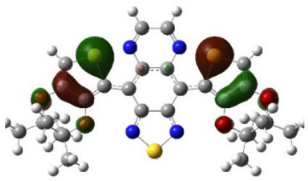	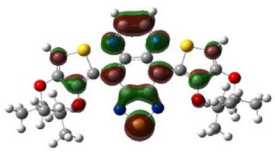
P6a	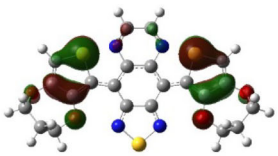	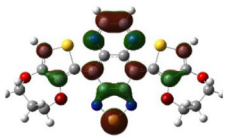
P6b	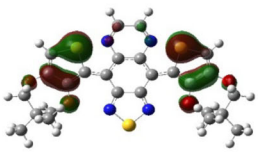	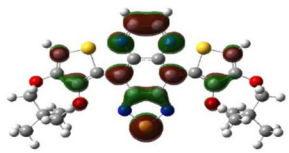
P6c	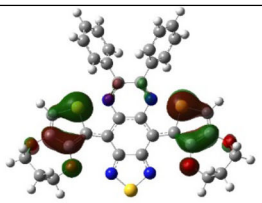	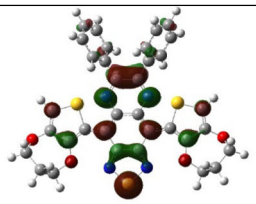

Table 3 Calculated orbital energies (eV), HOMO–LUMO energy gaps (eV), excitation energies (eV), binding energies (eV), oscillator strengths, maximum wavelengths, λ_{max} (nm), and HOMO-LUMO transitions of all compounds (B3LYP/6-31G(d,p))

	n	E_{HOMO} (eV)	E_{LUMO} (eV)	E_g (eV)	E_{exc} (eV)	E_b (eV)	λ_{max} (nm)	f	HOMO→LUMO transitions
P1a	1	− 5.19	− 3.73	1.46	1.29	0.17	958	0.172	91 → 92
	Exp.	− 5.32	− 3.96	1.47 (O)[a]; 1.49 (E)[a] 1.48 (O)[b,c];1.36[d]					
	B3LYP/cc-PVTZ[e]	− 5.34	− 3.70	1.64	1.43	-		-	
	6-31G(d)[f]	-	-	1.56	1.41	0.15		0.201	
	2	− 4.89	− 3.86	1.03	0.99	0.04	1254	0.839	181 → 182
	3	− 4.78	− 3.93	0.85	0.81	0.04	1550	1.660	271 → 272
	4	− 4.72	− 3.97	0.75	0.7	0.05	1774	2.513	361 → 362
	5	− 4.69	− 3.99	0.7	0.62	0.07	1992	3.325	451 → 452
	6	− 4.66	− 4.01	0.66	0.57	0.09	2155	4.113	541 → 542
	∞			0.51					
	Exp.[b,c]			0.5 (O)					
P1b	1	− 5.17	− 3.51	1.65	1.20	0.16	1001	0.17	107 → 108
	2	− 5.11	− 3.54	1.57	1.24	0.27	1032	0.405	213 → 214
	3	− 5.12	− 3.54	1.58	1.17	0.29	1061	0.696	319 → 320
	4	− 4.99	− 3.59	1.39	1.13	0.29	1093	0.811	425 → 426
	5	− 4.96	− 3.59	1.36	1.14	0.30	1090	1.222	531 → 532
	∞			1.37					
P2a	1	− 4.68	− 3.33	1.36	1.21	0.15	1026	0.191	121 → 122
	Exp.[g]			1.6 (O)					
	2	− 4.28	− 3.41	0.87	0.90	− 0.03	1377	0.871	241 → 242
	3	− 4.13	− 3.46	0.67	0.72	− 0.05	1690	1.667	361 → 362
	4	− 4.04	− 3.49	0.55	0.60	− 0.05	2005	2.618	481 → 482
	5	− 3.83	− 3.77	0.06	0.03	0.03	1220	0.013	601 → 602
	6	− 3.84	− 3.76	0.09	0.01	0.04	1265	0.002	721 → 722
	∞	− 3.82	− 3.78	0.1					
	Exp.[h]			0.5 (O); 0.88 (E)					
P2b	1	− 4.69	− 3.28	1.4	1.21	0.19	1015	0.200	153 → 154
	2	− 4.37	− 3.39	0.99	0.89	0.10	1140	0.546	305 → 306
	3	− 4.19	− 3.48	0.71	0.59	0.12	1190	0.321	457 → 458
	4	− 3.73	− 3.64	0.08	0.10	− 0.01	754	0.069	609 → 610
	5	− 3.72	− 3.66	0.06	0.03	0.03	1270	0.012	761 → 762
	∞			0.05					
P3a	1	− 4.54	− 3.22	1.32	1.19	0.13	1038	0.203	129 → 130
	2	− 4.23	− 3.33	0.90	0.91	− 0.01	1350	0.862	257 → 258
	3	− 4.10	− 3.40	0.70	0.73	− 0.03	1670	1.640	385 → 386
	4	− 3.85	− 3.76	0.09	0.14	− 0.05	1145	0.135	513 → 514
	5	− 1.01	− 0.94	0.07	0.12	− 0.06	1110	0.183	641 → 642
	∞			0.05					
P3b	1	− 4.89	− 3.40	1.49	1.20	0.14	1031	0.211	145 → 146
	2	− 4.37	− 3.57	0.81	0.79	0.02	1345	0.458	289 → 29
	3	− 3.96	− 3.76	0.20	0.31	− 0.13	785	0.315	433 → 434
	4	− 3.85	3.75	0.10	0.12	− 0.03	950	0.092	577 → 578
	5	− 3.80	− 3.74	0.06	0.04	0.02	1260	0.022	721 → 722
	∞			0.29					
P4a	1	− 5.23	− 3.44	1.8	1.51	0.29	820	0.171	90 → 91
	Exp.			1.80(E)[c];2.00 (O)[g]					
	2	− 4.89	− 3.56	1.34	1.16	0.18	1071	0.797	179 → 180
	3	− 4.77	− 3.61	1.16	0.98	0.18	1265	1.456	268 → 269
	4	− 4.71	− 3.64	1.08	0.88	0.20	1411	2.079	357 → 358
	5	− 4.68	− 3.66	1.03	0.79	0.18	1568	3.043	446 → 447
	6	− 4.66	− 3.67	0.99	0.78	0.22	1600	3.301	535 → 536
	∞			0.84					
	Exp.[c,i]			0.7 (O)					
P4b	1	− 5.18	− 3.30	1.87	1.20	0.67	1034	0.106	106 → 107
	2	− 4.95	− 3.36	1.58	1.18	0.40	1050	0.062	211 → 212
	3	− 4.87	− 3.38	1.48	1.14	0.34	1099	0.03	316 → 317
	4	− 4.83	− 3.39	1.44	1.09	0.35	1135	0.802	421 → 422
	∞			1.3					
P5a	1	− 4.71	− 3.18	1.53	1.21	0.33	1028	0.104	120 → 121

Table 3 (continued)

	n	E_{HOMO} (eV)	E_{LUMO} (eV)	E_g (eV)	E_{exc} (eV)	E_b (eV)	λ_{max} (nm)	f	HOMO→LUMO transitions
	2	−4.38	−3.29	1.1	0.96	0.14	1295	0.581	239 → 240
	3	−4.18	−3.35	0.83	0.75	0.08	1653	1.240	358 → 359)
	4	−4.05	−3.31	0.75	0.64	0.1	1925	1.550	477 → 478
	5	−4.04	−3.32	0.72	0.60	0.12	2060	1.897	596 → 597
	∞			0.51					
	Exp.[c]			0.7 (O)					
P5b	1	−4.59	−3.09	1.5	1.18	0.33	1054	0.110	152 → 153
	2	−4.47	−3.28	1.2	0.86	0.1	1225	0.679	303 → 304
	3	−3.98	−3.23	0.75	0.69	0.06	1580	1.279	454 → 455
	4	−3.89	−3.26	0.63	0.58	0.05	1830	2.030	605 → 606
	5	−3.83	−3.28	0.56	0.51	0.05	1930	2.733	756 → 757
	6	−3.79	−3.29	0.5	0.44	0.06	2333	3.048	907 → 908
	∞			0.35					
P6a	1	−4.60	−3.10	1.5	1.24	0.26	955	0.147	128 → 129
	2	−4.23	−3.20	1.03	0.94	0.09	1320	0.773	255 → 256
	3	−4.09	−3.26	0.83	0.77	0.07	1618	1.474	382 → 383
	4	−4.01	−3.29	0.73	0.66	0.07	1883	2.277	509 → 510
	5	−3.97	−3.31	0.66	0.58	0.08	2125	3.062	636 → 637
	6	−3.94	−3.32	0.62	0.53	0.09	2315	3.846	763 → 764
	∞			0.45					
P6b	1	−4.64	−3.14	1.5	1.24	0.27	950	0.152	144 → 145
	2	−4.26	−3.24	1.02	0.91	0.28	960	0.129	287 → 288
	3	−4.12	−3.30	0.82	0.29	−0.12	810	0.279	457 → 458
	4	−4.05	−3.34	0.71	0.11	−0.02	1150	0.093	609 → 610
	5	−3.78	−3.68	0.09	0.03	0.03	1270	0.014	761 → 762
	∞			0.19					
P6c	1	−4.77	−2.91	1.85	1.52	0.33	814	0.134	168 → 169
	2	−4.29	−2.96	1.32	1.10	0.23	1128	0.622	335 → 336
	3	−4.09	−2.97	1.12	0.91	0.21	1367	1.193	502 → 503
	4	−3.88	−3.02	0.86	0.71	0.15	1748	1.972	669 → 670
	5	−3.83	−3.03	0.8	0.64	0.16	1923	2.605	836 → 837
	∞			0.6					

E band gap measured electrochemically, *O* band gap measured optically

[a] Taken from Ref [12]

[b] Taken from Ref [13]

[c] Taken from Ref [14]

[d] Taken from Ref [15]

[e] Taken from Ref [24]

[f] Taken from Ref [23]

[g] Taken from Ref [16]

[h] Taken from Ref [17]

[i] Taken from Ref [18]

planar structures. Another result is that the polymer, **P6c**, in which there are two phenyl rings at the 6- and 7-positions of the quinoxaline, has a large HOMO-LUMO gap due to the steric hindrance of the phenyl groups.

To show the accuracy and reliability of the method used in the calculation, computed E_g values were compared with experimental data and previous calculation results. There are experimental band gap values in the literature for polymers **P1a**, **P2a**, **P4a**, and **P5a**. As can be seen in Table 3, experimental E_g values for **P1a**, **P2a**, **P4a**, and **P5a** are 0.5, 0.5, 0.7, and 0.7 eV, respectively, and corresponding energy gap values are 0.51, 0.1, 0.84, and 0.51 eV. On the other hand, theoretically calculated energy gaps of the studied polymers, except P**1a**, are not included in the literature. The HOMO-LUMO energy gap computed with B3LYP/6-31G(d) for **P1a** is 0.98 eV. The energy gaps computed with the B3LYP/6-31G(d,p) level are quite compatible with the experimental band gap values. Zhang and Musgrave stated that HOMO, LUMO, and HOMO-LUMO gap values predicted by hybrid functionals such as O3LYP, B3LYP, and B1B95

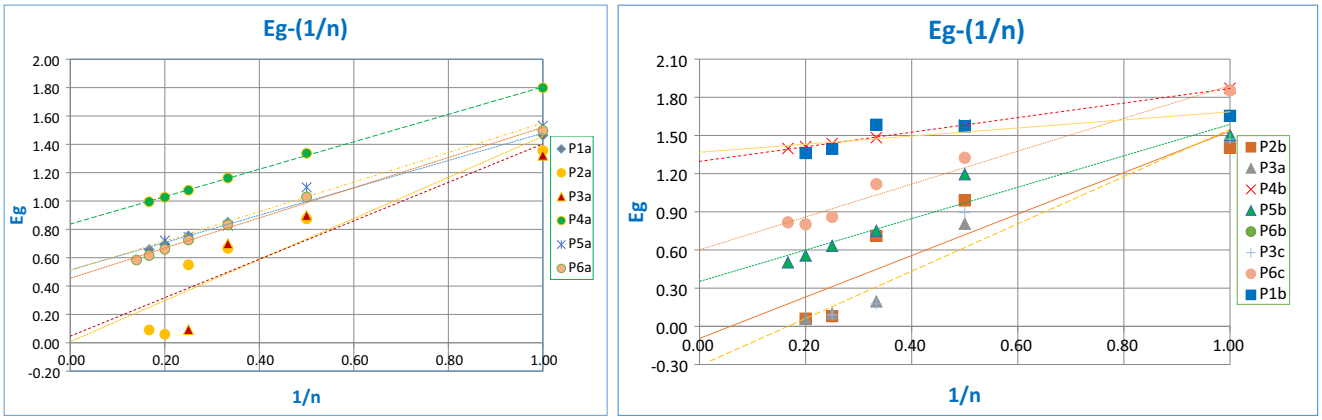

Fig. 7 HOMO-LUMO energy gap (E_g) as a function of reciprocal polymer length ($1/n$) where n is the number of monomer units

are better than those predicted by non-hybrid functionals with the pure DFT methods [36]. They also stated that the TD-DFT method is more suitable than the pure DFT method for predicting the LUMO, HOMO, and HOMO-LUMO gap. In order to compare the results of the two methods and test the reliability of our calculation results, we performed our calculations with the TD-DFT method. Our prediction results using both methods showed that the HOMO, LUMO, and HOMO-LUMO gap values of our highly conjugated molecules are the same. In addition, there is a high linear correlation between DFT-HOMO-LUMO gaps and TD-DFT first excitation energies for the studied compounds (Fig. 5S in Supporting Information). Thus, it can be concluded that the B3LYP/6-31G(d,p) level of theory is a good approach to compute the HOMO-LUMO energy gap of BBT, TQ, and similar type of copolymers. We can also conclude that BBT and TQ derivatives can be good candidates in electronic applications with their improved optical and electronic properties.

UV analysis

The properties of a conjugated polymer relate to the energy gap (E_g). The excited energy (E_{exc}) of a molecule is the minimum energy required for an electronic transition and the lowest transition energy corresponds to the transition from HOMO to LUMO. The exciton binding energy (E_b), which allows excitons to separate into electrons and holes in the donor, is defined as the difference between the energy gap (E_g) and E_{exc} [37]. Therefore, it is possible to estimate E_b from TD-DFT calculations. To determine the absorption properties of the monomers and oligomers studied, UV-Vis spectra of all compounds were simulated using the TDDFT at the B3LYP/6-31G (d,p) level from their pre-optimized structures. The computed UV–Vis absorption spectra of the monomers and oligomers are presented in Fig. 8 and the absorption wavelengths (λ_{max}), oscillator strengths (f), excitation energies (E_{exc}), and exciton binding energies (E_b) of all monomers and oligomers are given in Table 3. According to the UV simulation results, two absorption bands are observed in the near-infrared region in all monomers, but larger oligomers have only a wide absorption band in the red region. All the lowest energy electronic transitions and the maximum absorption considered here correspond to the transition from HOMO to LUMO in all oligomers.

The substituted BBT derivatives have been shown to have NIR absorption and experimental maximum absorption reported for the monomer **P1a** is in the wavelength region longer than 700 nm [21, 24]. In general, there is a bathochromic shift by increased oligomer length from monomer to the larger oligomer. However, it was observed that maximum absorption wavelengths of tetramer and pentamer of the **P2a**, **P2b**, **P3a**, and **P3b** oligomers were reduced.

As seen from Table 3, the absorption wavelengths of the BBT derivatives are bigger than those of corresponding TQ monomers. The calculated maximum absorption wavelengths of the TQ derivatives decrease in the following order: ProDOT > EDOT > TH. The exciton binding energies (E_b) of the BBT derivatives are smaller than those of corresponding TQ monomers. Low E_b value is required for conjugated material applications such as photovoltaic. It can be concluded that BBT acceptors are better candidates than their TQ-based counterparts for photovoltaic applications.

Conclusions

DFT and TDDFT methods were used to compute the geometric, optical, and electronic properties of a series of D-A-D type polymers composed of benzobisthiadiazole and thiadiazoloquinoxaline units symmetrically bonded to two

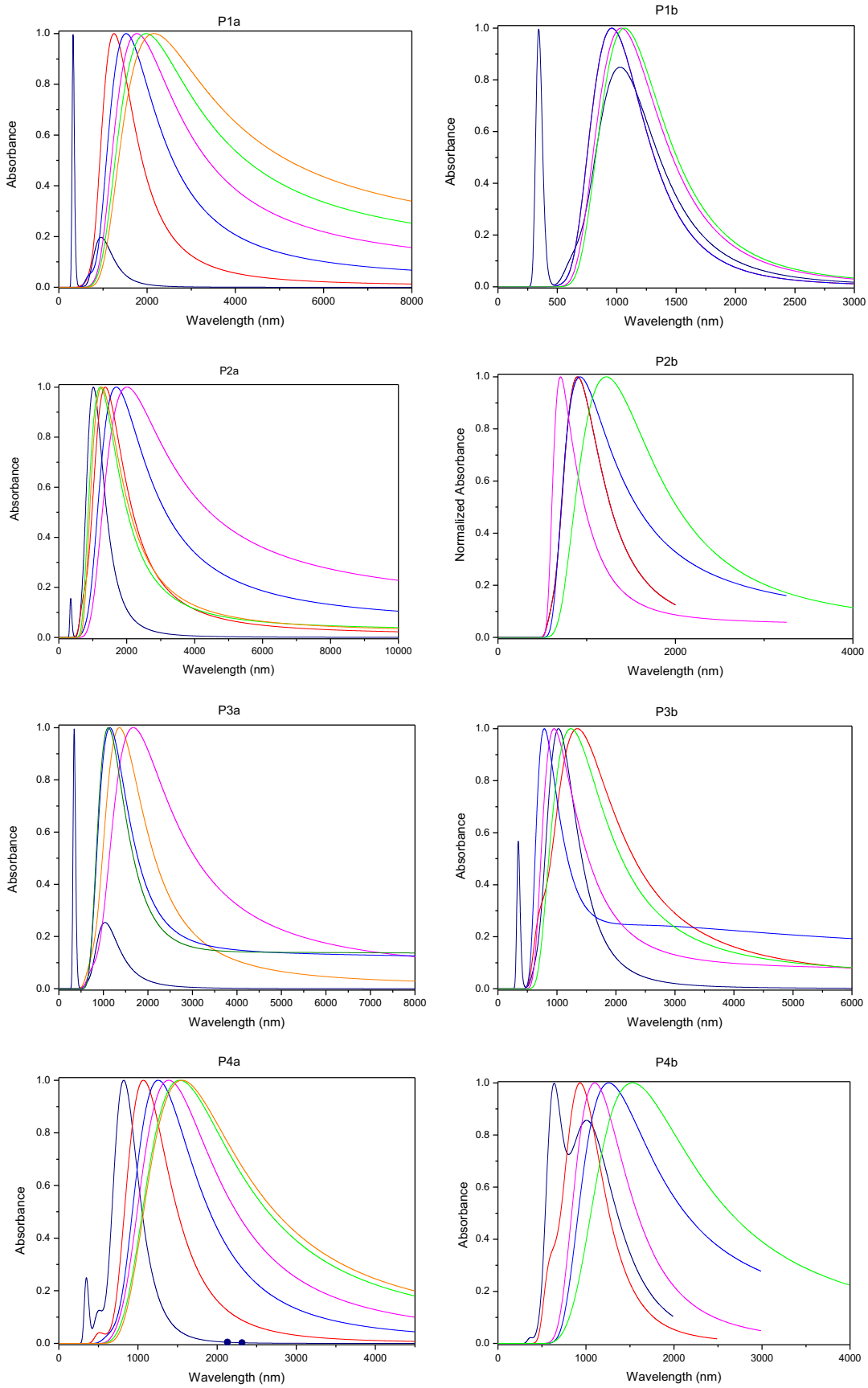

Fig. 8 UV–visible absorption spectra of all monomers and oligomers obtained from TDDFT/B3LYP/6-31G(d,p) simulations

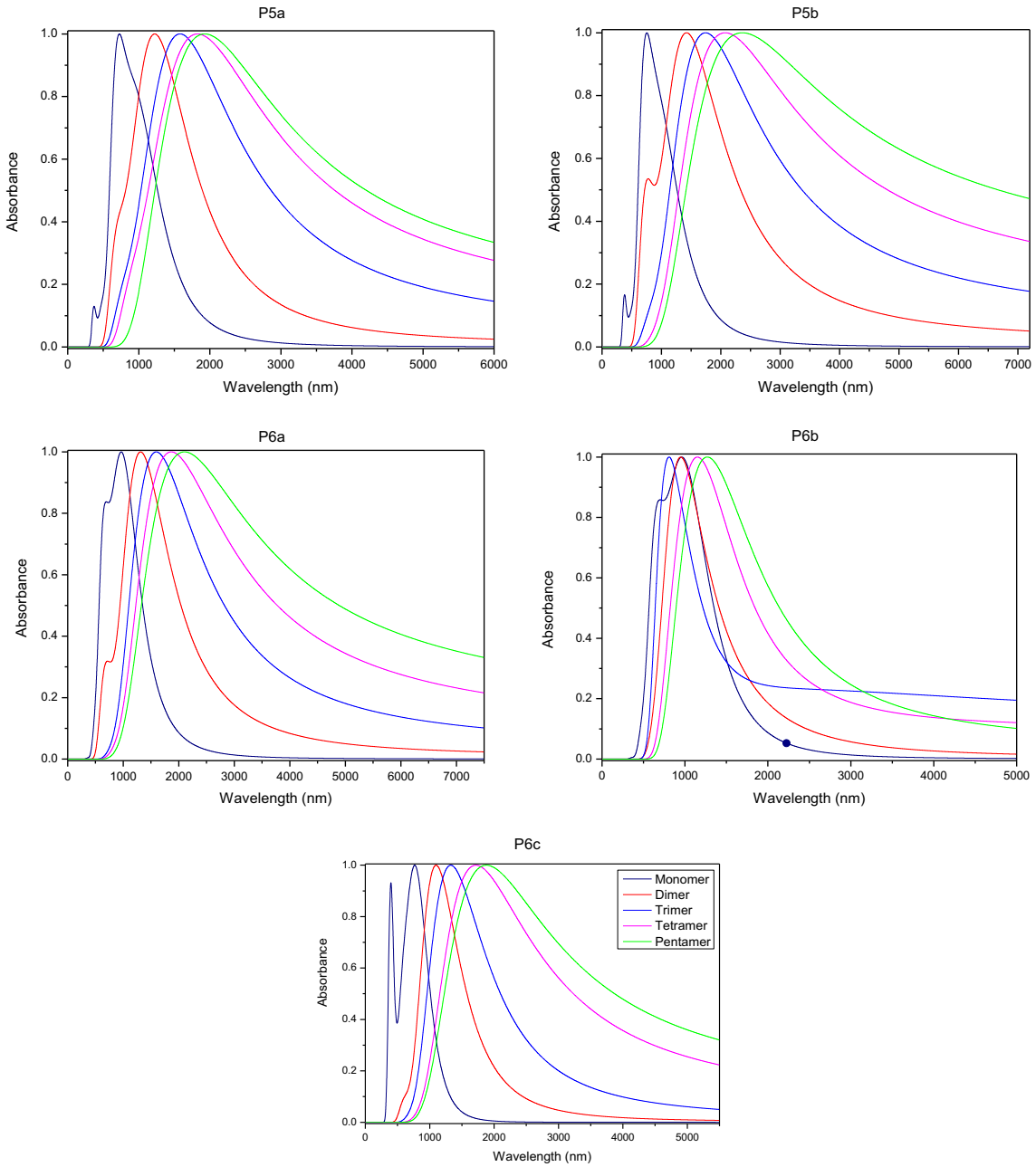

Fig. 8 (continued)

THs, EDOTs or ProDOTs. The calculated HOMO-LUMO gaps of the examined oligomers were in the range of 0.05–1.37 eV and there is good agreement with the experimental values. The calculation results show that the large increase in the dihedral angle increases the energy gap. The steric effect or electron donor effect of methyl groups may cause the energy to either increase or decrease. BBT copolymers have smaller energy gap than the TQ copolymers. On the other hand, the energy gap of EDOT or ProDOT-containing polymers is lower than the TH-containing derivatives. UV-Vis spectra of all compounds were calculated by the TDDFT at the B3LYP/6-31G (d,p) level in the gas phase. Two absorbance bands are observed in all studied monomers in the NIR region while larger oligomers have only one wide absorption band in the red region. The novel BBT acceptors with improved optical and electronic properties are a good candidate than their TQ-based counterparts for photovoltaic applications.

Acknowledgments We would like to thank Erol Eroğlu (Akdeniz University) who supported us with computer facilities in our calculations, especially with large oligomers such as pentamer and hexamer.

References

1. Qian G, Li X, Wang ZY (2009) Visible and near-infrared chemosensor for colorimetric and ratiometric detection of cyanide. J. Mater. Chem. 19:522–530. https://doi.org/10.1039/b813478b
2. Mikroyannidis JA, Tsagkournos DV, Sharma SS, Vijay YK, Sharma GD (2011) Low band gap conjugated small molecules containing benzobisthiadiazole and thienothiadiazole central units: synthesis and application for bulk heterojunction solar cells. J. Mater. Chem. 21:4679–4688. https://doi.org/10.1039/c0jm03436c
3. Bundgaard E, Krebs FC (2006) Low-band-gap conjugated polymers based on thiophene, benzothiadiazole, and benzobis(thiadiazole). Macromolecules 39:2823–2831. https://doi.org/10.1021/ma052683e
4. Tam TL, Li H, Wei F, Tan KJ, Kloc C, Lam YM, Mhaisalkar SG (2010) One-pot synthesis of 4,8-dibromobenzo- [1,2-c;4,5-c′]bis[1,2,5]thiadiazole. Org. Lett. 12:3340–3343. https://doi.org/10.1021/ol100989v
5. Keshtov ML, Marochkin DV, Kochurov VS, Khokhlov AR, Koukaras EN, Sharma GD (2014) New conjugated alternating benzodithiophene-containing copolymers with different acceptor units: synthesis and photovoltaic application. J. Mater. Chem. A 2:155–171. https://doi.org/10.1039/c3ta12967e
6. Patel DG, Feng F, Ohnishi YY, Abboud KA, Hirata S, Schanze KS, Reynolds JR (2012) It takes more than an imine: the role of the central atom on the electron-accepting ability of benzotriazole and benzothiadiazole oligomers. J. Am. Chem. Soc. 134:2599–2612. https://doi.org/10.1021/ja207978v
7. Yang Y, Farley RT, Steckler TT, Eom SH, Reynolds JR, Schanze KS, Xue J (2008) Near-infrared organic light-emitting devices based on donor-acceptor-donor oligomers. Appl. Phys. Lett. 93:163305. https://doi.org/10.1063/1.3006059
8. Ellinger S, Graham KR, Shi P, Farley RT, Steckler TT, Brookins RN, Taranekar P, Mei J, Padilha LA, Ensley TR, Hu H, Webster S, Hagan DJ, Van Stryland EW, Schanze KS, Reynolds JR (2011) Donor-acceptor-donor-based π-conjugated oligomers for nonlinear optics and near-IR emission. Chem. Mater. 23:3805–3817. https://doi.org/10.1021/cm201424a
9. Yamashita Y, One K, Tomura M, Tanaka S (1997) Synthesis and properties of Benzobis(thiadiazole)s with nonclassical n-e1ectron ring systems. Tetrahedron 53:10169–10178
10. Keshtov ML, Toppare L, Marochkin DV, Kochurov VS, Parashchuk DY, Trukhanov VA, Khokhlov AR (2013) Synthesis and photovoltaic properties of new donor-acceptor benzodithiophene-containing copolymers. Polym Sci Ser B 55:360–372. https://doi.org/10.1134/S1560090413060055
11. Tam TLD, Salim T, Li H, Zhou F, Mhaisalkar SG, Su H, Lam YM, Grimsdale AC (2012) From benzobisthiadiazole, thiadiazoloquinoxaline to pyrazinoquinoxaline based polymers: effects of aromatic substituents on the performance of organic photovoltaics. J. Mater. Chem. 22:18528–18534. https://doi.org/10.1039/c2jm33317a
12. Li H, Tam TL, Lam YM, Mhaisalkar SG, Grimsdale AC (2011) Synthesis of low band gap [1,2,5]-thiadiazolo[3,4-g]quinoxaline and pyrazino[2,3-g]quinoxaline derivatives by selective reduction of benzo[1,2-c;4,5-c′]bis[1,2,5]thiadiazole. Org. Lett. 13:46–49. https://doi.org/10.1021/ol102465a
13. Karikomi M, Kitamura C, Tanaka S, Yamashita Y (1995) New narrow-bandgap polymer composed of benzobis(1,2,5-thiadiazole) and thiophenes. J. Am. Chem. Soc. 117:6791–6792. https://doi.org/10.1021/ja00130a024
14. Kitamura C, Tanaka S, Yamashita Y (1996) Design of narrow-bandgap polymers syntheses and properties of monomers and polymers containing aromatic-donor and o-quinoid-acceptor units. Chem. Mater. 8:570–578
15. Kono T, Kumaki D, Nishida JI, Tokito S, Yamashita Y (2010) Dithienylbenzobis(thiadiazole) based organic semiconductors with low LUMO levels and narrow energy gaps. Chem. Commun. 46:3265–3267. https://doi.org/10.1039/b925151k
16. Yang Y, Farley RT, Steckler TT, Eom SH, Reynolds JR, Schanze KS, Xue J (2009) Efficient near-infrared organic light-emitting devices based on low-gap fluorescent oligomers. J. Appl. Phys. 106:044509. https://doi.org/10.1063/1.3204947
17. Steckler TT, Abboud KA, Craps M, Rinzler AG, Reynolds JR (2007) Low band gap EDOT-benzobis(thiadiazole) hybrid polymer characterized on near-IR transmissive single-walled carbon nanotube electrodes. Chem. Commun. 46:4904–4906. https://doi.org/10.1039/b709672k
18. Kitamura C, Tanaka S, Yamashita Y (1996) New narrow-bandgap polymers composed of [1,2,5]thiadiazolo[3,4-g]quinoxaline and aromatic heterocycles. Chem. Lett. 25:63–64. https://doi.org/10.1246/cl.1996.63
19. Ono K, Tanaka S, Yamashita Y (1994) Benzobis(thiadiazole)s containing hypervalent sulfur atoms: novel heterocycles with high electron affinity and short intermolecular contacts between heteroatoms. Angew Chemie Int Ed English 33:1977–1979. https://doi.org/10.1002/anie.199419771
20. Tarsang R, Jungsuttiwong S, Vao-soongnern V (2016) Computational calculations of substitution pattern effects on the optical properties of benzobis(thiadiazole) derivatives as near-infrared-emitting organic compounds. Comput Theor Chem 1098:31–40. https://doi.org/10.1016/j.comptc.2016.10.018
21. Thomas A, Bhanuprakash K, Prasad KMMK (2011) Near-infrared absorbing benzobis(thiadiazole) derivatives: computational studies point to biradical nature of the ground states. J. Phys. Org. Chem. 24:821–832. https://doi.org/10.1002/poc.1845
22. Fu Y, Shen W, Li M (2011) Molecular design and density functional theory investigation of novel low-band-gap copolymers between quinoid acceptors and aromatic donors. Polym. Int. 60:211–221. https://doi.org/10.1002/pi.3094
23. Köse ME (2012) Evaluation of acceptor strength in thiophene coupled donor-acceptor chromophores for optimal design of organic photovoltaic materials. J. Phys. Chem. A 116:12503–12509. https://doi.org/10.1021/jp309950f
24. Thomas A, Chaitanya GK, Bhanuprakash K, Prasad KMMK (2011) Substituents destabilize the molecule by increasing biradicaloid character and stabilize by intramolecular charge transfer in the derivatives of benzobis(thiadiazole) and thiadiazolothienopyrazine: a computational study. ChemPhysChem 12:3458–3466. https://doi.org/10.1002/cphc.201100701
25. Garcia M, Fomina L, Fomine S (2010) Electronic structure evolution of neutral and dicationic states of conjugated polymers with their band gap. Synth. Met. 160:2515–2519. https://doi.org/10.1016/j.synthmet.2010.09.037
26. Civcir PÜ (2018) Computational modeling of donor-acceptor-donor conjugated polymers based on benzothiadiazole. Comput Theor Chem 1128:70–82. https://doi.org/10.1016/j.comptc.2018.02.013
27. Frisch MJ, Trucks GW, Schlegel HB, Scuseria GE, Robb M, Cheeseman JR, Scalmani G, Barone V, Mennucci B, Petersson GA, Nakatsuji H, Caricato M, Li X, Hratchian HP, Izmaylov AF, Bloino J, Zheng G, Sonnenberg JL, Hada M, Ehara M, Toyota K, Fukuda R, Hasegawa FDGA, Salvador P, Dannenberg JJ, Dapprich S, Daniels AD, Farkas Ö, Foresman JB, Ortiz JV, Cioslowski J

(2009) Gaussian 09, Revision D.01. Gaussian, Inc., Wallingford. https://doi.org/10.1159/000348293
28. Dennington R, Keith T, Millam J (2009) GaussView, Version 5.0.8.: Semichem Inc., Shawnee Mission KS
29. Stewart JJP (2007) Optimization of parameters for semiempirical methods V: modification of NDDO approximations and application to 70 elements. J. Mol. Model. 13:1173–1213. https://doi.org/10.1007/s00894-007-0233-4
30. Hohenberg P, Kohn W (1964) The inhomogeneous electron gas. Phys. Rev. 136:B864. https://doi.org/10.1103/PhysRevB.7.1912
31. Kohn W, Sham LJ (1965) Self-consistent equations including exchange and correlation effects. Phys. Rev. A140:1133–A1138. https://doi.org/10.1103/PhysRev.140.A1133
32. Lee C, Yang W, Parr RG (1988) Development of the Colle-Salvetti correlation-energy formula into a functional of the electron density. Phys. Rev. B 37:785–789. https://doi.org/10.1103/PhysRevB.37.785
33. Becke AD (1988) Density-functional exchange-energy approximation with correct asymptotic-behavior. Phys. Rev. A 38:3098–3100. https://doi.org/10.1103/PhysRevA.38.3098
34. Ditchfield R, Hehre WJ, Pople JA (1971) Self-consistent molecular-orbital methods. IX. An extended Gaussian-type basis for molecular-orbital studies of organic molecules. J Chem Phys 54:724–728. https://doi.org/10.1063/1.1674902
35. Pai CL, Liu CL, Chen WC, Jenekhe SA (2006) Electronic structure and properties of alternating donor-acceptor conjugated copolymers: 3,4-ethylenedioxythiophene (EDOT) copolymers and model compounds. Polymer 47:699–708. https://doi.org/10.1016/j.polymer.2005.11.083
36. Zhang G, Musgrave CB (2007) Comparison of DFT methods for molecular orbital eigenvalue calculations. J. Phys. Chem. A 111:1554–1561. https://doi.org/10.1021/jp061633o
37. Dkhissi A (2011) Excitons in organic semiconductors. Synth Met 161:1441–1443. https://doi.org/10.1016/j.synthmet.2011.04.003